Journal of Hazardous Materials 166 (2009) 1180–1185

Contents lists available at ScienceDirect

Journal of Hazardous Materials

journal homepage: www.elsevier.com/locate/jhazmat

Adsorption of *p*-nitroaniline from aqueous solutions onto activated carbon fiber prepared from cotton stalk

Kunquan Li[a,b], Zheng Zheng[a,*], Jingwei Feng[a], Jibiao Zhang[a], Xingzhang Luo[a], Guohua Zhao[a], Xingfa Huang[a]

[a] *State Key Laboratory of Pollution Control and Resource Reuse, School of the Environment, Nanjing University, Nanjing 210093, China*
[b] *Nanjing Agricultural University, Nanjing 210031, China*

ARTICLE INFO

Article history:
Received 16 January 2008
Received in revised form
21 September 2008
Accepted 4 December 2008
Available online 9 December 2008

Keywords:
Activated carbon fiber
p-Nitroaniline
Adsorption isotherm
Kinetics

ABSTRACT

Activated carbon fiber prepared from cotton stalk was used as an adsorbent for the removal of *p*-nitroaniline (PNA) from aqueous solutions. Liquid phase adsorption experiments were conducted and the maximum adsorptive capacity was determined. The effect of experimental parameters such as pH, salinity and temperature on the adsorption was studied. The obtained experimental data were then fitted with the Langmuir, Freundlich and Redlich-Peterson models to describe the equilibrium isotherms. The kinetics rates were modeled by using the pseudo-first-order and pseudo-second-order equations. The results indicated that cotton stalk activated carbon fiber (CS-ACF) is an effective adsorbent for the removal of PNA from aqueous solutions. The maximum adsorption capacity of 406 mg g^{-1} was achieved at the initial PNA concentration of 200 mg L^{-1}. The optimum pH for the removal of PNA was found to be 7.6. The presence of ammonium chloride proved to be favorable for the process of adsorption. The adsorption amount decreased with increasing temperature. The Redlich-Peterson model was found to best represent the equilibrium data. The kinetic data followed closely the pseudo-second-order equation. Thermodynamic study showed the adsorption was a spontaneous exothermic physical process.

1. Introduction

p-Nitroaniline (PNA) is an important compound used as an intermediate or precursor in the manufacture of organic synthesis such as azo dyes, antioxidants, fuel additives, corrosion inhibitors, pesticides, antiseptic agents, medicines for poultry and the synthesis of pharmaceuticals. However, the presence of PNA in water, even at very low concentrations, is extremely harmful to aquatic life and human health in terms of its hematoxicity, splenotoxicity and nephrotoxicity [1,2]. Therefore it has been listed as one of the major priority contaminants in water for removal by many countries including China.

Some treatment technologies such as advanced oxidation process [3–5], extraction [6] and biodegradation [7] have been used to remove PNA from industrial wastewaters. Unfortunately they have proved to be inefficient, costly and usually cause secondary pollution. Due to the presence of a nitro group in the aromatic ring, PNA is resistant to chemical and biological oxidation degradation, and the anaerobic degradation produces nitroso and hydroxylamines compounds which are known as carcinogenic [7,8]. Therefore, the purification of wastewater polluted with PNA is a great challenge to environmental scientists and engineers, and new cost-effective technologies for PNA removal are crucial for today's world.

Adsorption is widely used because of its relatively simple design, easy operation and relatively simple regeneration. Varieties of adsorbents [9–11] have been tried to remove PNA from wastewaters. However, there are few reports that activated carbon fiber (ACF), the most widely used adsorbent, was used as an adsorbent for the purification of wastewater polluted with PNA. ACF has many favorable characteristics such as a high specific surface area, excellent mechanical integrity and high mass transfer rates [12,13]. Moreover, ACF is easier to be handled in a batch adsorber than granular and powdered activated carbon [13]. Thus, it has received increasing attention in recent years as an adsorbent for water treatment [12–15].

The aim of this study was to study the utility of cotton stalk activated carbon fiber (CS-ACF), a low cost as well as non-hazardous material, as an adsorbent for PNA removal from aqueous solutions by static batch experiments. The effects of experimental parameters such as pH, ammonium chloride and temperature were investigated. Furthermore, isotherm, thermodynamic and kinetic studies were also carried out.

* Corresponding author. Tel.: +86 25 83593109 fax: +86 25 83707304.
E-mail address: zzheng@nju.edu.cn (Z. Zheng).

0304-3894/$ – see front matter.
doi:10.1016/j.jhazmat.2008.12.035

2. Experimental

2.1. Adsorbent

2.1.1. Preparation of adsorbent

The precursor used for the production of ACF was cotton stalk fiber provided by Hubei Chemical Fiber Co., China. A horizontal tubular furnace with an artificial intelligence temperature controller AI708P and a 60 cm tubular ceramic insert was used for the production of the ACF. Raw cotton stalk fiber was impregnated with a 4% potassium dihydrogen phosphate solution with a mass ratio of 1:60 and stirred for 20 min. Then the mixed precursors were filtered and dried in an oven at 105 °C. After that, 10 g of the mixed precursors were placed in a 10 cm stainless steel container, and the steel container was positioned in the center of tubular ceramic insert in the horizontal tubular furnace. Stabilization was carried out by heating to 250 °C at a rate of 10 °C min^{-1} under a constant high purity nitrogen flow of 80 cm^3 min^{-1} and by maintaining the temperature for 30 min. The carbonization was then carried out by raising the temperature at a rate of 10 °C min^{-1} to 600 °C, and maintaining the temperature for 30 min. Thereafter, the gas flow was switched to a water steam and activation was carried out at 850 °C for 20 min. At last, the activated product was cooled to room temperature under a nitrogen flow.

2.1.2. Pretreatment of adsorbent

The CS-ACF was boiled and washed three times in distilled water. It was dried at 105 °C for 24 h before being used as an adsorbent. The specific surface area of CS-ACF was measured with a Micrometics ASAP-2020 surface area measurement instrument (Micromeritics Instrument, Norcros, USA) following the BET method. The pH level at the point of zero charge (pH_{pzc}) of CS-ACF was determined by a batch equilibrium method described by Babic [16]. The elemental analysis of CS-ACF was obtained from a CHN-O-Rapid Elemental Analytical Instrument (Elementer, Germany). The characteristics of CS-ACF are: BET surface area, 1520 m^2 g^{-1}; total pore volume, 1.2 cm^3 g^{-1}; micropore volume, 0.89 cm^3 g^{-1}; average pore width, 1.96 nm; bulk, 0.04 g cm^{-3}; pH_{pzc}, 4.9. And the percentages of C, H and O in CS-ACF are 81.67%, 1.31% and 17.02%, respectively.

2.2. Chemicals

All the reagents used were of analytical reagent grade and without further purification. The chemicals used in this study, i.e., potassium dihydrogen phosphate, hydrochloric acid, sodium hydroxide, ammonium chloride and PNA, were purchased from Shanghai Chemical Reagent Co., China. The PNA solution (200 mg L^{-1}) was prepared by dissolving the required amount of PNA in distilled water in the adsorption test.

2.3. Adsorption studies

In batch adsorption experiments, different doses of adsorbent (0.1–1.0 g L^{-1}) were added into several 250 mL Erlenmeyer flasks, each containing 100 mL solution (200 mg L^{-1} PNA) at 298, 308 and 318 K, respectively, in order to determine the adsorption isotherms and to evaluate the effect of temperature on PNA adsorption. Following this, the flasks were shaken at 150 rpm at a pre-settled temperature for 48 h in a constant temperature shaker (Shanghai Scientific Instrument Co. Ltd., China). Samples were filtrated, and then the concentrations of PNA at equilibrium (C_e) were determined.

The effect of pH levels on the adsorption of PNA onto CS-ACF was studied by adjusting the pH levels of PNA solutions between 2.0 and 12.0 with dilute HCl or NaOH solution at 298 K, and with the dose of adsorbent being 0.30 g L^{-1}. The APHS-2C pH meter (Shanghai Kangyi Instrument Co., China) was used to measure the pH levels of the solutions. The effect of ammonium chloride on the adsorption was studied with the pH level at 7.6 at 298 K, and with the dose of adsorbent being 0.30 g L^{-1}.

In kinetic studies, batch experiments were conducted at different periods by adding 0.2415 g adsorbent into each 500 mL PNA solution at 298, 308 and 318 K, respectively. Samples were collected periodically at every 5 min for the first 30 min and then at every 15 min for kinetic studies.

The amount of PNA adsorbed per unit mass of adsorbent at equilibrium (q_e) was calculated according to the following equation:

$$q_e = \frac{V(C_0 - C_e)}{W} \quad (1)$$

where C_0 and C_e are the initial and equilibrium concentrations of PNA (mg L^{-1}), respectively, V is the volume of the solution (L), and W is the mass of adsorbent (g).

2.4. Analysis

The concentrations of PNA were analyzed by using a Helious Betra UV–vis spectrometer (Unicam Co., UK). A standard PNA solution was taken and the absorbance was determined at different wavelengths to obtain a plot representing the absorbance versus wavelength. The wavelength corresponding to maximum absorbance as determined from this plot was 381 nm. This wavelength was used for preparing the calibration curve between absorbance and the concentration of the PNA solution. The results showed that the calibration curve of the absorbance was linear with the PNA concentration in the range of 0.25–20 mg L^{-1} (R^2 = 0.9999). In order to prevent pH from affecting absorbency of PNA samples, all samples were basified to a pH level of 8.0 by addition of 0.1 M sodium hydroxide.

3. Results and discussion

3.1. Effect of pH on adsorption

The pH of a solution is one of the most important parameters affecting the adsorption process. In fact, solution pH would affect both aqueous chemistry and surface binding sites of the adsorbent. Moreover, a change in pH also results in a change in charge profile of adsorbate species, which consequently influences the interactions between the adsorbate species and adsorbent [17,18].

The effect of pH on PNA adsorption onto the CS-ACF is depicted in Fig. 1 including the PNA dissociation curve dependent upon solution pH. As shown in Fig. 1, the PNA adsorption onto CS-ACF

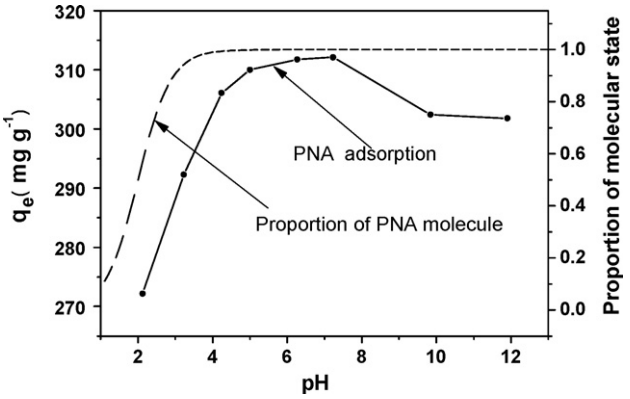

Fig. 1. Effect of pH on the PNA adsorption (left) and the proportion of PNA molecule (right), (V, 100 mL; C_0, 200 mg L^{-1}; CS-ACF dose, 0.30 g L^{-1}; T, 298 K; agitation rate, 150 rpm; contact time, 48 h; solution pH 2–12).

was observed at an optimum pH of 7.6. Below and above this pH, a decreasing trend in the adsorption was observed. The equilibrium adsorption amount of PNA q_e increased sharply from 272 to 307 mg g^{-1} at an initial PNA concentration of 200 mg L^{-1} with the solution pH increasing from 2 to 5, then increased slightly from 307 to 311 mg g^{-1} with a further increase in range pH from 5 to 7.6. These results should be attributed to the electrostatic interactions between the PNA and the surface of CS-ACF. PNA (R-NH_2) gets protonated in acidic medium, and the protonated PNA becomes more and more deprotonated in higher pH from Eq. (2).

$$RNH_2 + H^+ \rightleftharpoons RNH_3^+ \quad (2)$$

As solution pH was lower than 4.9, the net charge on the surface of CS-ACF was positive since the pH_{pzc} was found to be 4.9. With the increase of solution pH, PNA cations became more and more deprotonated, and the net charges on the surface of CS-ACF decreased. Hence, the electrostatic repulsions decreased rapidly with the solution pH increasing from 2 to 4.9, which caused the increase of PNA adsorption amount. When the solution pH was higher than 4.9, the surface of CS-ACF was negatively charged. So electrostatic attractions between the adsorbent and PNA anions occurred, which was responsible for the slight increase of PNA adsorption amount in the pH range 5–7.6. The decrease of PNA adsorption amount from 311 to 301 mg g^{-1} with the solution pH increasing from 7.6 to 12 could result from two possible reasons. In competitive adsorption experiments, the adsorbent surface is initially populated by the smaller molecules, and then these adsorbed molecules must be displaced by other molecules of higher molecular weight [19]. So it could be speculated that the OH^- ions were initially adsorbed on the surface of the adsorbent in basic medium, and adsorption of PNA required the desorption of OH^- ions. In addition, there might be a slight repulsion between surface negative charge and lone electron pairs of PNA [20].

3.2. Effect of ammonium chloride on adsorption

The effect of ammonium chloride on adsorption is depicted in Fig. 2. As shown in Fig. 2, the equilibrium adsorption amount q_e increased with the increase of ammonium chloride concentration. Furthermore, the equilibrium adsorption amount displayed a linear correlation with the concentration of ammonium chloride, which was in accord with the research results of Turner [21]. And this phenomenon was due to the salting-out effect. The ions of ammonium and chloride dissociated from ammonium chloride molecules were hydrated with many water molecules, which thus resulted in the decrease of the water molecules available for dissolution of PNA. Hence, the presence of ammonium chloride enhanced the

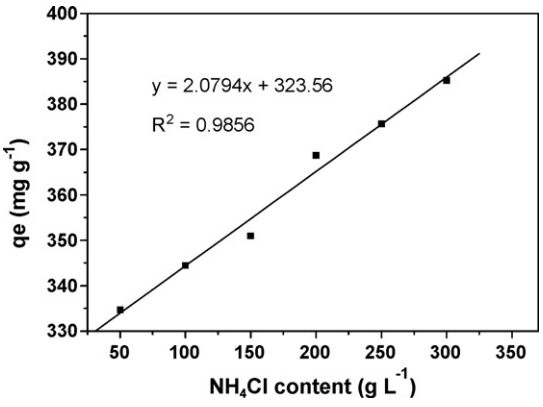

Fig. 2. Effect of ammonium chloride on the PNA adsorption (V, 100 mL; C_0, 200 mg L^{-1}; solution pH, 7.6; CS-ACF dose, 0.30 g L^{-1}; T, 298 K; agitation rate, 150 rpm; contact time, 48 h).

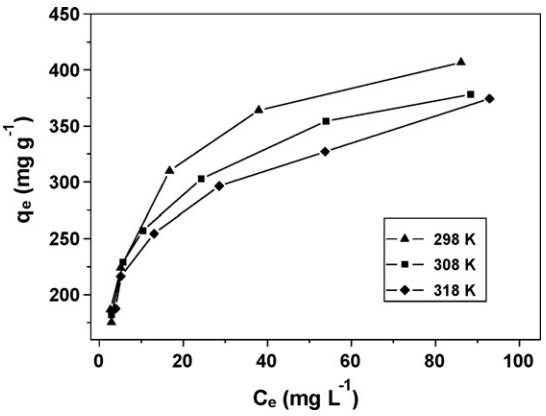

Fig. 3. Effect of temperature on the PNA adsorption (V, 100 mL; C_0, 200 mg L^{-1}; solution pH 7.6; CS-ACF dose, 0.10–1.0 g L^{-1}; T, 298 K; agitation rate, 150 rpm; contact time, 48 h).

PNA hydrophobic action, which was in favor of adsorption [22]. Tang reported a similar result that the adsorption capacity for *p*-nitrophenol on activated carbon fiber increased with the increase in the salt concentration of sodium chloride [23].

3.3. Effect of solution temperature on PNA adsorption

Graphic presentations of PNA adsorption at the experimental temperature of 298 K, 308 K, and 318 K are shown in Fig. 3. Fig. 3 shows that the equilibrium adsorption amount q_e decreased with increasing temperature, indicating that the adsorption was an exothermic process. Furthermore, the equilibrium adsorption amount q_e decreased greatly with increasing temperature when the solution equilibrium concentration was higher than 30 mg L^{-1}, but changed slightly with temperature when the solution equilibrium concentration was lower than 10 mg L^{-1}. This phenomenon indicated the heterogeneity of the adsorption sites on CS-ACF surface. Generally, more active sites are initially occupied by the adsorbates, and then less active sites. From Eq. (3), the fractional surface coverage of the adsorbent is in proportion to the equilibrium adsorption concentration [24].

$$\theta = \frac{bC_e}{1 + bC_e} \quad (3)$$

where θ is the fractional surface coverage, b is the Langmuir model constant, and C_e is the equilibrium concentration of PNA in the solution (mg L^{-1}). As a result, fewer of more active sites on the surface of CS-ACF were available in higher equilibrium adsorption concentration. Therefore, the PNA molecules with higher kinetic energy at higher temperature were easier to escape from the surface of CS-ACF to the aqueous solution.

3.4. Adsorption isotherms

The experimental results were fitted with the well-known models of Langmuir, Freundlich and Redlich-Peterson in order to understand the adsorption mechanisms of PNA onto CS-ACF. It is well known that the Langmuir model is usually used with an ideal assumption of an entirely homogeneous adsorption surface, whereas the Freundlich model is appropriate for a heterogeneous surface. The Redlich-Peterson isotherm model, the combinations of the Langmuir and Freundlich, is applicable in describing microporous adsorption. These isotherm equations are given in Table 1.

Since the three parameters of the Redlich-Peterson isotherm model can be estimated effectively using non-linear regression, the software Origin (version 7.0) was used to determine the parameters of the three isotherm models for the comparison. Different

Table 1
Isotherm models adopted in this work and their parameters.

Isotherm	Model	Parameters
Langmuir	$q_e = \frac{bq_0C_e}{1+bC_e}$	C_e: equilibrium liquid phase concentration ($mg\,L^{-1}$) q_e: equilibrium adsorption capacity ($mg\,g^{-1}$) b: constant of Langmuir ($L\,mg^{-1}$); q_0: the maximum adsorption capacity ($mg\,g^{-1}$)
Freundlich	$q_e = k_F C_e^{1/n}$	k_F: the Freundlich constant for a heterogeneous adsorbent n: related to the magnitude of the adsorption driving force and to the adsorbent site energy distribution
Redlich-Peterson	$q_e = \frac{K_1C_e}{1+aC_e^{\beta}}$	k_1: constant of Redlich-Peterson ($L\,mg^{-1}$); a: constant of Redlich-Peterson $(L\,mg^{-1})^g$; β: constant of Redlich-Peterson

adsorption isotherms obtained at various temperatures are illustrated in Fig. 4. The values of the parameters and the correlation coefficients obtained at various temperatures are listed in Table 2. By comparing the correlation coefficients (R^2) for the three models at different temperatures, it can be inferred that both the empirical Freundlich model and Redlich-Peterson model are better than Langmuir model in describing the adsorption of PNA onto CS-ACF. It is revealed that the energy distribution for the adsorption "sites" was of essentially an exponential type [25], rather than of the uniform type. In this case, some sites were highly energetic and bound the adsorbed PNA strongly, whereas some were much less energetic and bound PNA weakly, which resulted in the possibility of more than one monomolecular layer of coverage on the CS-ACF surface.

From Table 2, the maximum adsorption capacity of PNA onto CS-ACF was more than 406 $mg\,g^{-1}$ at initial PNA concentration of 200 $mg\,L^{-1}$ at 25 °C. The adsorption capacities of PNA on other adsorbents such as clinoptilolit, humic acid and XAD-4 polymeric resin were found to be 0.85, 1.8 and 318 $mg\,g^{-1}$, respectively [9–11]. When compared to these adsorbents, CS-ACF had the largest capacity for the removal of PNA. Further more, the values of $1/n$ were found to be less than 1 for all temperatures, indicating that the adsorption was favorable [26]. The results above suggested that CS-ACF was an effective adsorbent for the purification of wastewater polluted with PNA.

3.5. Thermodynamic study

The thermodynamic parameters including change in the Gibbs free energy (ΔG°), enthalpy (ΔH°), and entropy (ΔS°) were determined by using the following equations [27–28]:

$$\Delta G^\circ = \frac{\Delta H^\circ - T\,\Delta S^\circ}{R} \quad (4)$$

$$\ln C_e = \left(\frac{\ln q_e - \Delta S^\circ}{R}\right) + \frac{\Delta H^\circ}{RT} \quad (5)$$

where q_e is the amount of PNA adsorbed per unit mass of adsorbent at equilibrium ($mg\,L^{-1}$), C_e is the equilibrium concentration of PNA in the solution ($mg\,L^{-1}$), R is the gas constant (8.314 $J\,mol^{-1}\,K^{-1}$) and T is the absolute temperature (K). At different temperatures (298–318 K), the corresponding C_e values for different fixed q_e were calculated by the appropriate Redlich-Peterson model isotherms. Thus, ΔH° and ΔS° were obtained from the slope and intercept of the line plotted by $\ln C_e$ versus $1/T$, respectively, as shown in Fig. 5. The correlation coefficients (R^2) for the linear equations were 0.9709, 0.9938 and 0.9985, respectively. Related thermodynamic parameters are summarized in Table 3.

The change of Gibbs free energy (ΔG°) for the physical adsorption is generally in the range of nil to −20 $kJ\,mol^{-1}$, and that for the chemical adsorption is in the range of −80 to −400 $kJ\,mol^{-1}$ [29]. As shown in Table 3, the overall free energy change during the adsorption process was in the range of −4.16 $kJ\,mol^{-1}$ to −8.91 $kJ\,mol^{-1}$ for the experimental range of temperatures.

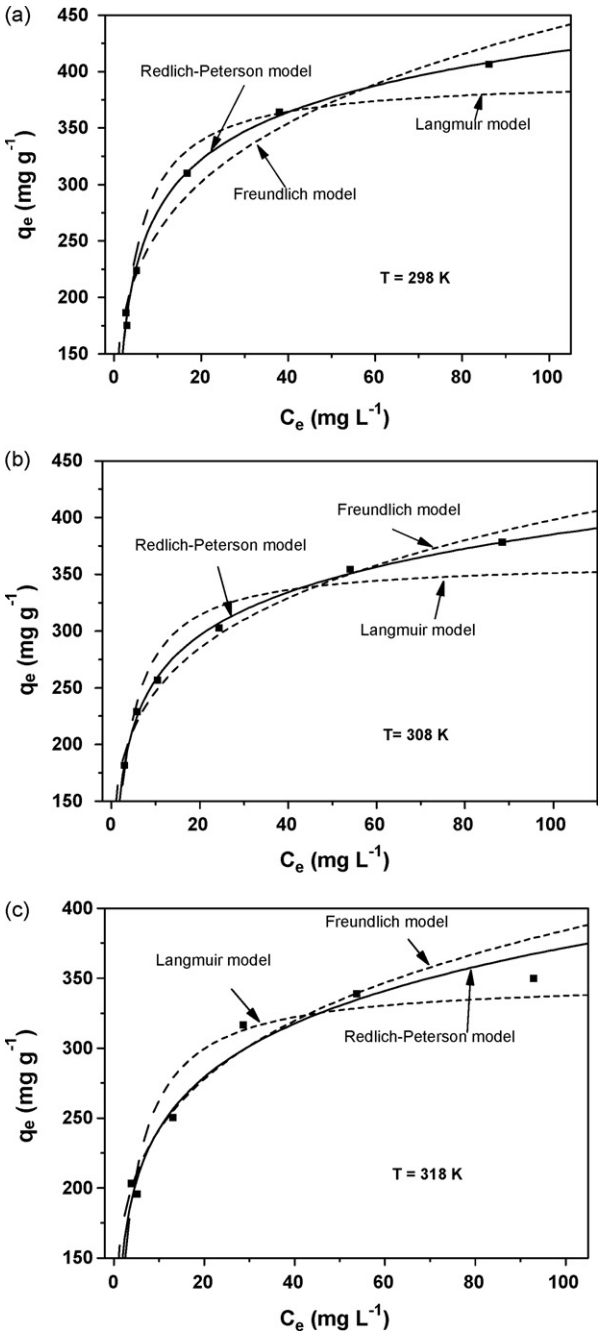

Fig. 4. Comparison of different isotherm models for PNA adsorption on CS-ACF at different solution temperatures.

Table 2
Isotherm parameters for PNA adsorption onto CS-ACF at various temperatures.

Temperature (K)	$q_{e,exp}$ (mg g^{-1})	Langmuir model			Freundlich model			Redlich-Peterson model			
		q_0	b	R^2	k_F	n	R^2	k_l	a	β	R^2
298	406.5	394.10	0.30752	0.96753	152.07	4.3624	0.9739	181.16	0.7253	0.8839	0.9963
308	378.2	361.74	0.32994	0.93205	153.12	4.8200	0.9866	250.27	1.1901	0.8652	0.9979
318	364.3	348.48	0.30616	0.93154	152.13	4.9694	0.9870	329.13	1.8106	0.8421	0.9911

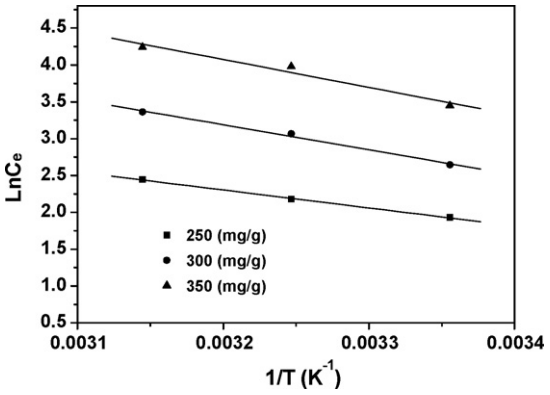

Fig. 5. Plot of $\ln C_e$ versus $1/T$ for estimation of thermodynamic parameters for the adsorption of PNA onto CS-ACF.

Table 3
Thermodynamic data for adsorption of PNA onto CS-ACF evaluated at different equilibrium adsorption amounts and different temperatures.

q_e (mg g^{-1})	ΔH° (kJ mol^{-1})	ΔS° (J mol^{-1} K^{-1})	ΔG° (kJ mol^{-1})		
			298 K	308 K	318 K
250	−20.24	−38.02	−8.91	−8.53	−8.15
300	−28.28	−69.60	−7.54	−6.85	−6.15
350	−31.43	−90.40	−5.88	−5.02	−4.16

The results demonstrated that the discussed adsorption was a spontaneous physical process and that the system had not gained energy from an external source. Furthermore, the absolute value of ΔG° decreased with the increase of the equilibrium adsorption amount, as well as the increase of temperature on the same adsorption amount, indicating a decrease in adsorption impetus. Both phenomena suggested that the reverse process of adsorption, desorption, can be easily carried out on the condition of a larger equilibrium adsorption amount and a higher temperature.

The negative enthalpy change (ΔH°) values indicated that the adsorption was an exothermic process [30]. In addition, the absolute value of ΔH° decreased with the increase of the equilibrium adsorption amount, further confirming the experimental observation that the adsorption amount increased with the decrease of temperature. The adsorption entropy changes (ΔS°) were less than zero, which was accorded with the fact that the mobility of adsorbates on adsorbent surface becomes more restricted as compared with that of those in solution.

3.6. Adsorption kinetics

The pseudo-first-order and pseudo-second-order equations were applied to model the kinetics of PNA adsorption onto CS-ACF. The pseudo-first-order rate expression of Langergren [31] is presented as:

$$\frac{dq}{dt} = k_1(q_e - q_t) \tag{6}$$

Integrating Eq. (6) with respect to integration conditions $q_t = 0$ to $q_t = q_t$ at $t = 0$ to $t = t$, the kinetic rate expression becomes

$$q_t = q_e - q_e\, e^{-k_1^t} \tag{7}$$

where q_e is the amount of PNA adsorbed per unit mass of adsorbent at equilibrium (mg g^{-1}), q_t is the amount of PNA adsorbed at various times t (mg g^{-1}), and k_1 is the rate constant of pseudo-first-order kinetic model (g mg^{-1} min^{-1}).

The pseudo-first-order rate constant k_1 and the equilibrium adsorption amount q_e were obtained though non-linear regression fitting, and the related kinetic parameters are summarized in Table 4. As shown in Table 4, the corresponding coefficients (R^2) for the first-order kinetic model at different temperatures were all lower than 0.92. And the calculated q_e values, 314.99, 280.72 and 270.71 mg g^{-1} respectively, for three temperatures of 298 K, 308 K and 318 K from the pseudo-first-order kinetic model, were far lower than the corresponding experimental q_e value, 342.91, 327.24 and 303.51 mg g^{-1}. It was also found that the variation in rate was not proportional to the solution temperature. These results indicated that the pseudo-first-order kinetic model was not appropriate to describe the adsorption process.

And the pseudo-second-order kinetic model [32–34] is expressed as:

$$\frac{dq}{dt} = k_2(q_e - q_t)^2 \tag{8}$$

Integrating Eq. (8) for the boundary conditions $q_t = 0$ to $q_t = q_t$ at $t = 0$ to $t = t$ is simplified as:

$$\frac{t}{q_t} = \frac{1}{(k_2 q_e^2)} + \frac{t}{q_e} \tag{9}$$

where q_e is the amount of PNA adsorbed per unit mass of adsorbent at equilibrium (mg g^{-1}), q_t is the amount of PNA adsorbed at various times t (mg g^{-1}), and k_2 is the second-order rate constant (g mg^{-1} min^{-1}). As shown in Fig. 6, the q_e and the second-order rate constant k_2 could be determined from the plot of t/q_t versus t from Eq. (9). And the related kinetic parameters are summarized in Table 4. The correlation coefficients (R^2) for the linear equations

Table 4
Parameters of two kinetic models for adsorption of PNA onto CS-ACF.

Temperature (K)	$q_{e,exp}$ (mg g^{-1})	Pseudo-first-order model			Pseudo-second-order model		
		q_e (mg g^{-1})	K_1 (min^{-1})	R^2	q_e (mg g^{-1})	K_2 (min^{-1})	R^2
298	342.91	314.99	0.03436	0.9170	344.83	1.46E−04	0.9997
308	327.24	280.72	0.02101	0.9100	322.58	7.81E−05	0.9981
318	303.51	270.71	0.02263	0.9092	312.50	9.41E−05	0.9987

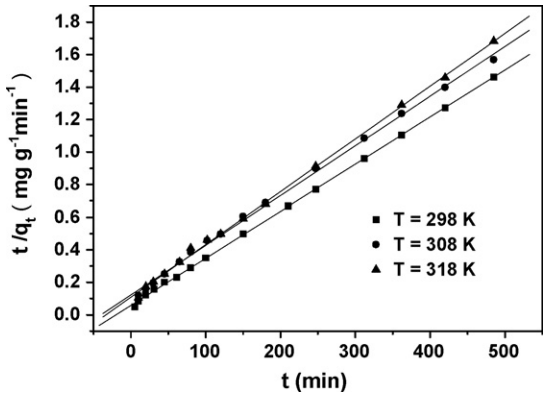

Fig. 6. Pseudo-second-order kinetic plots for the adsorption of PNA onto CS-ACF at different solution temperatures (V, 500 mL; C_0, 200 mg L^{-1}; CS-ACF dose, 0.4830 g L^{-1}; solution pH 7.6; agitation rate, 150 rpm).

were 0.9997, 0.9981 and 0.9987, respectively. The pseudo-second-order rate constant (k_2) decreased with increasing temperature. And the calculated q_e values agreed very well with the experimental values. These results indicated that the pseudo-second-order kinetic model was appropriate for the entire adsorption process.

4. Conclusion

The present study indicated that the cotton stalk activated carbon is an effective adsorbent for the removal of PNA from aqueous solutions. The adsorption was found to be greatly dependent on solution pH, temperature and salinity. The adsorption capacity decreased with increasing temperature. The optimal solution pH level was determined to be 7.6. The maximum adsorption capacity of PNA onto CS-ACF was more than 406 mg g^{-1} at initial PNA concentration of 200 mg L^{-1} at 25 °C. The Langmuir, Freundlich and Redlich-Peterson models were used to interpret the adsorption phenomenon of the adsorbate, and the results implied that the surface of CS-ACF was heterogeneous. The pseudo-first-order and pseudo-second-order kinetic models were used to test the kinetic data. The pseudo-second-order kinetic model was found to be appropriate for the entire adsorption process. The negative values of free energy changes (ΔG°) and enthalpy changes (ΔH°) for the adsorption indicated that the adsorption was a spontaneous exothermic physical process.

Acknowledgement

The authors thank the Natural Science Foundation of China (No. 10475040) and Nanjing Agricultural University Youth Science & Technology Innovation Foundation (China) for financial support.

References

[1] F. Bhunia, N.C. Saha, A. Kaviraj, Effects of aniline—an aromatic amine to some freshwater organisms, Ecotoxicology 12 (2003) 397–403.
[2] K.T. Chung, S.C. Chen, Y.Y. Zhu, Toxic effects of some benzamines on the growth of *Azotobacter vinelandii* and other bacteria, Environ. Toxicol. Chem. 16 (1997) 1366–1369.
[3] D.S. Lee, K.S. Park, Y.W. Nam, et al., Hydrothermal decomposition and oxidation of *p*-nitroaniline in supercritical water, J. Hazard. Mater. 56 (1997) 247–256.
[4] J.H. Sun, S.P. Sun, M.H. Fan, A kinetic study on the degradation of *p*-nitroaniline by Fenton oxidation process, J. Hazard. Mater. 148 (2007) 172–177.
[5] S. Gautam, S.P. Kamble, S.B. Sawant, et al., Photocatalytic degradation of 4-nitroaniline using solar and artificial UV radiation, Chem. Eng. J. 110 (2005) 129–137.
[6] L.R. Shen, P.Z. Yang, L.Y. Chen, Treatment of waster water containing *p*-nitrophenylamine with emulsion liquid membrane processs, Tec. Water Tr. (Chinese) 23 (1997) 45–49.
[7] A. Saupe, High-rate biodegradation of 3- and 4-nitroaniline, Chemosphere 39 (1999) 2325–2346.
[8] M.A. Oturan, J. Peiroten, P. Chartrin, A.J. Acher, Complete destruction of *p*-nitrophenol in aqueous medium by electro-Fenton method, Environ. Sci. Technol. 34 (2000) 3474–3479.
[9] K. Zheng, B.C. Pan, Q.J. Zhang, Enhanced adsorption of *p*-nitroaniline from water by a carboxylated polymeric adsorbent, Sep. Purif. Technol. 57 (2007) 250–256.
[10] Y.Q. Wu, M. Zhou, M.G. Ma, et al., Adsorption kinetics of *p*-nitroaniline on the insolubilized humic acid, Tec. Water. Tr. (Chinese) 33 (2007) 14–17.
[11] M.G. Ma, Y.X. Wei, Y. Zhang, et al., Modify of clinoptilolit (from Baiyin) and its adsorption of *p*-nitroaniline, J. Anhui Agri. Sci. (Chinese) 35 (2007) 2061–2062.
[12] M. Suzuki, Activated carbon fiber: fundamentals and applications, Carbon 32 (1994) 577–586.
[13] C. Brasquet, P. Le Cloriec, Adsorption onto activated carbon fibers: application to water and air treatments, Carbon 35 (1997) 1307–1313.
[14] I. Martin-Gulloan, R. Font, Dynamic pesticide removal with activated carbon fibers, Water Res. 35 (2001) 516–520.
[15] P.A. Quinlivan, L. Li, D.R.U. Knappe, Effects of activated carbon characteristics on the simultaneous adsorption of aqueous organic micropollutants and natural organic matter, Water Res. 39 (2005) 1663–1673.
[16] B.M. Babic, S.K. Milonjic, M.J. Polovina, et al., Point of zero charge and intrinsic equilibrium constants of activated carbon cloth, Carbon 37 (1999) 477–481.
[17] Y. Hu, G.J. Liu, H.H. Xu, et al., Adsorption Action, first ed., Shanghai Technology Literature Publishing Company (Chinese), 1989.
[18] A. Ornek, M. Ozacar, I.A.S. engil, Adsorption of lead onto formaldehyde or sulphuric acid treated acorn waste: equilibrium and kinetic studies, Biochem. Eng. J. 37 (2007) 192–200.
[19] E. Lutanie, J.C. Voegel, P. Schaaf, M. Freund, J.P. Cazenave, A. Schmitt, Competitive adsorption of human immunoglobulin G and albumin: consequences for structure and reactivity of the adsorbed layer, Proc. Natl. Acad. Sci. U.S.A. 89 (1992) 9890–9894.
[20] Osman Duman, Erol Ayranci, Structural and ionization effects on the adsorption behaviors of some anilinic compounds from aqueous solution onto high-area carbon-cloth, J. Hazard. Mater. B120 (2005) 173–181.
[21] A. Turner, M.C. Rawling, Influence of salting out on the sorption of neutral organic compounds in estuaries, Water. Res. 35 (2001) 4379–4389.
[22] Z.Q. Huang, Guide Discuss of Electrolyte Solutions, Beijing Technology Publishing Company, China (Chinese), 1987.
[23] D.Y. Tang, Z. Zheng, K. Lin, et al., Adsorption of *p*-nitrophenol from aqueous solutions onto activated carbon fiber, J. Hazard. Mater. 143 (2007) 49–56.
[24] M.A. Hasnat a, M.M. Uddin a, A.J.F. Sameda, et al., Adsorption and photocatalytic decolorization of a synthetic dye erythrosine on anatase TiO_2 and ZnO surfaces, J. Hazard. Mater. 147 (2007) 471–477.
[25] D.O. Cooney, Adsorption Design for Wastewater Treatment, Lewis Publishers, USA, 1999.
[26] S.D. Faust, O.M. Aly, Adsorption Processes for Water Treatment, Butterworths, London, 1987.
[27] E. Tutem, R. Apak, C.F. Unal, Adsorptive removal of chlorophenols from water by bituminous shale, Water Res. 32 (1998) 2315–2324.
[28] S.S. Gupta, K.G. Bhattacharyya, Adsorption of Ni(II) on clays, J. Colloid. Interface Sci. 295 (2006) 21–32.
[29] Y. Wang, Y. Mu, Q.B. Zhao, et al., Isotherms, kinetics and thermodynamics of dye biosorption by anaerobic sludge, Sep. Purif. Technol. (Chinese) 50 (2006) 1–7.
[30] M. Karaa, H. Yuzera, E. Sabah, Adsorption of cobalt from aqueous solutions onto sepiolite, Water Res. 37 (2003) 224–232.
[31] S. Lagergren, About the theory of so-called adsorption of soluble substances, Kungliga Svenska Vetenskapsakademiens Handlingar 24 (1898) 1–39.
[32] Y.S. Ho, Adsorption of heavy metals from waste streams by peat, Ph.D. thesis, University of Birmingham, Birmingham, UK, 1995.
[33] Y.S. Ho, G. McKay, Comparative sorption kinetic studies of dye and aromatic compounds onto fly ash, J. Environ. Sci. Health. A 34 (1999) 1179–1204.
[34] Y.S. Ho, Comment on Adsorption of naphthalene on zeolite from aqueous solution by C.F. Chang, C.Y. Chang, K.H. Chen, W.T.T. sai, J.L. Shie, Y.H. Chen, J. Colloid. Interface Sci. 283 (2005) 274–277.